Particles Interaction Influence on Plume Divergence in Plasma Thruster Magnetic Nozzle

IEPC-2015-356／ISTS-2015-b-356

Presented at Joint Conference of 30th International Symposium on Space Technology and Science 34th International Electric Propulsion Conference and 6th Nano-satellite Symposium, Hyogo-Kobe, Japan July 4 – 10, 2015

Alena Kitaeva[1], Haibin Tang[2], Min Li[3] and Guangnan Chen[4]
Beihang University, Beijing, 100191, China

Abstract: Due to the plasma quasi-neutrality the momentum received by the oppositely charged particles from the applied electric field is partially compensated. It is only the difference between electrons and ions velocities that contributes to the electric field acceleration mechanism in some plasma thrusters. In the analysis of the plume detachment in the magnetic nozzle systems of non-electrodless thrusters the studies are usually focused on particles interaction with the magnetic field, both induced and applied. Conversely, the interaction between charged particles and electric field has received far less attention. The simulation results presented in this paper demonstrate how the space distribution of the electric potential influences the plasma exhaust velocity radial distribution. We suggest that a possible reason for efficiency loses in the magnetic nozzle systems is the difference between axial and peripheral particles velocities caused by electric force non-uniformity. The importance of a simulating the AF-MPDTs ionization chamber and magnetic nozzle combined is also emphasized.

Nomenclature

B	=	magnetic induction field
E	=	electric field
e	=	elementary charge, electron index
i	=	ion index
$I(x,y,z)$	=	three dimensional current
H	=	Hall index
f_V	=	viscous body force
j	=	current density, same type particles index
k	=	different type particles index
m	=	particle mass
M_A	=	Alfven Mach number
n	=	number density
p	=	pressure
q	=	particle charge
r	=	radial position for cylindrical coordinate system, radial index
R_L	=	Larmor radius
S	=	Swirl index

[1] PhD student, School of Astronautics, Bee-Aynil@yandex.ru.
[2] Professor, School of Astronautics, thb@buaa.edu.cn.
[3] PhD student, School of Astronautics, lm@buaa.edu.cn.
[4] Master Student, School of Electronic and Information Engineering, 304055353@qq.com

t	=	time
u	=	particle velocity
v_A	=	Alfven velocity
$v\perp$	=	velocity perpendicular to the magnetic field
x	=	positive x direction is perpendicular to the thruster axis on the model plane pointing right
y	=	positive y direction is along the thruster axis in the direction of the flow
z	=	z axis is pointing out of the model plane.
Z	=	charge number
β	=	kinetic parameter
θ	=	azimuthal index
μ_0	=	permeability of free space
ν	=	collision frequency
ρ	=	density
σ	=	electrical conductivity

I. Introduction

In the electric propulsion systems with applied magnetic field charged particles interact with the electric field, magnetic field, neutral particles, each other, the walls of the chamber, electrodes and outer space. The analysis and simulations of the each interaction type, both taken into consideration separately and in combination with others may help to understand the complex processes taking place in plasma thrusters and improve their efficiency.

Applied electric potential provides the fuel ionization for the arc-thrusters; however even for those applied-field magnetoplasmadynamic thrusters (AF-MPDT) with other ionization mechanisms the presence of the electric field improves thruster performance. The created current interacts with magnetic fields and provides accelerating momentum to the plasma flow.

The charged particles interaction with the magnetic field consists of the self-induced magnetic field part and applied magnetic field one. The self-field is induced azimuthally in the discharge area of the thruster from the axial component of the discharge current j_z. Its interaction with the current density produces the $\bar{j} \times \overline{B}$ body force, accelerating plasma downstream.

The main effect of the magnetic field applied parallel to the thruster axis on the plume is the flow collimation resulting in a better plume focusing and higher thrust. However, there is another way of applied magnetic field influencing on plasma. Even though the magnetic field itself does not add any energy to the flow it can cause the additional acceleration of plasma through putting it into rotation. The magnetic nozzle then converts the rotational energy of the flow into the thrust through the conservation of the angular momentum law. In most of the literature this acceleration mechanism is referred to as the Swirl acceleration. Plasma in the diverging magnetic field tends to behave in a similar to the gas flow in the gasdynamic nozzle. Sub-Alfvenic and super-Alfvenic regimes are recognized equivalently to subsonic and supersonic ones. Charged particles gyrate around the magnetic field lines. Electrons and ions move in opposite directions with different orbiting radius $R_L = m \cdot v_\perp / |q| B$ which is proportional to the particle mass m and velocity perpendicular to the magnetic field direction $V\perp$, and inverse proportional to magnetic field B. Due to their higher mass ion Larmor radius is sufficiently larger than electron one.

Hall currents generated in plasma also interact with the applied magnetic field resulting in so called Hall acceleration. Usually, the applied field effect on plasma plume is described through the interactions between the three dimensional current $I\ (x,y,\theta)$ and two dimensional magnetic field B (x,y): $J_\theta B_r$, $J_\theta B_z$, $J_z B_r$, $J_r B_z$ with a later two forming a force that may put plasma into rotation. The detailed description of how the rotational energy of plasma is converted into thrust can be found in Ref. 1. The azimuthal component of the current J_θ is usually considered to come entirely from the Hall effect in plasma. $J_\theta B_r$ force is the Hall acceleration force. The applied magnetic field also helps to protect electrodes from erosion.

The interspecies charged particles interactions like electron-ion, ion-neutral, electron-neutral play an important role in thruster processes. Particles interaction via collisions causes the momentum and energy exchange making plasma move as a whole. Sometimes charged particles-neutrals collisions may cause the charge exchange. The ambipolar electric field tends to provide plasma quasi-neutrality.

Ion-ion interactions and collisions between neutral particles are the cause of kinematic viscosity but they are often neglected, especially for MPDTs.

When particles contact with the chamber walls they may get neutralized, whereas their bombing of electrodes cause the erosion of latter and sufficient decrease of thruster operational time.

The combination of all these factors influencing plasma causes the complicated processes taking place in the thruster and downstream outside of it. The role of each interaction type in the plasma acceleration has been studied ever since electric propulsion invention. With the variation in plasma parameters some acceleration and focusing mechanisms benefit while others lose their efficiency. Therefore, it is always a matter of balancing, adjusting the values of electric potential, applied magnetic field strength and the geometry of the thruster to reach the optimal thrust efficiency for a particular objective.

Through experimental observations and analytical analysis the several critical parameters are added to those of hydrodynamics to be used in magnetohydrodynamics of electric propulsion. They are the magnetic Reynolds number R_{em}, the Hall number $\omega\tau$ and the Alfven (Stuart's) number S_{St}. In particular, R_{em} characterizes the fluid drifting in respect to the magnetic field, $\omega\tau$ represents the relation between Hall current and current parallel to the electric field, S_{St} shows the relation of the magnetic force to the inertia force. With $S_{St} > 1$ the applied magnetic field influence on plasma is sufficient. The detailed explanation of all these parameters can be found in Ref. 2. Some researchers suggest their own additional parameters to characterize certain regimes in plasma[3].

In the current work we investigate the electrons interaction with applied electric potential of different space distribution configurations in the presence of applied magnetic field. We analyze the impact of this interaction on the divergence of the plume and its detachment from the magnetic nozzle. Magnetic nozzles can be used with various types of electric thrusters and were experimentally proved to significantly improve their performance in some particular regimes. The main factor which imposes limitations on the applied magnetic field strength is the plume detachment problem.

As within the thruster the magnetic field lines are almost parallel to the thruster axis, particles, especially electrons, are forced to move parallel to the axis as well. However, outside of the thruster, magnetic field lines curve back to the coil guiding charged particles to follow them. While ions would escape easily due to their high mass and inertia, electrons may stay magnetized and may keep following the magnetic field lines. They may even pull ions with them. This particular particles' behavior causes an increase in the plume divergence and an efficiency drop. However, the majority of particles in most working regimes manage to escape. The main mechanisms which let this happen are believed to be resistive detachment, electron-inertia detachment and magnetic self-field detachment. These mechanisms were studied by many research groups[4-7]. Our work is mainly related to the electron-inertia detachment. According to it plasma manages to detach from a magnetic field lines when the flow velocity exceeds the local Alfven speed, so the kinetic energy of plasma becomes greater than the magnetic energy and $S_{St} < 1$ or:

$$\beta = \frac{\rho \cdot u^2/2}{B^2/(2 \cdot \mu_0)} = \left(\frac{u}{v_A} \right)^2 = M_A^2 \tag{1}$$

When β exceeds 1 plasma possess enough kinetic energy to detach from magnetic field lines.

The magnetic field is usually applied to the thruster through a magnetic coil placed around the acceleration channel. Depending on the thruster geometry and type, the number and position of coils may vary. Numerous configurations of the applied magnetic field have been studied in pursuit of the optimal magnetic field shape and strength[8,9].

Present work is mainly related to AF-MPD thrusters; however, its results might be extended to other types of non-electrodless thrusters.

II. AF-MPDT electrons - electric field interaction model

A. Forces acting on plasma in AF-MPDT.

In the AF-MPDT there is a cylindrical cathode situated on the axis of the chamber with coaxial anode around. The guiding magnetic field is applied axially. In this type of thruster plasma is usually just partially ionized and contains a significant part of neutral particles whose acceleration comes mostly from the collisions with charged particles. Electrons are accelerated in the applied electric potential field and transmit their momentum to ions mainly through collisions. Hall and Swirl acceleration mechanisms are believed to be the most significant ones[10-12]. The AF-MPDT has been extensively studied both experimentally and via simulations[13]. Various configurations were suggested, tested and analyzed (see Fig. 1). An extensive review of the work conducted in the field can be found in Ref. 14, while the theory of electric propulsion, the working principal and acting forces for MPD thrusters are well described in Ref. 15-17.

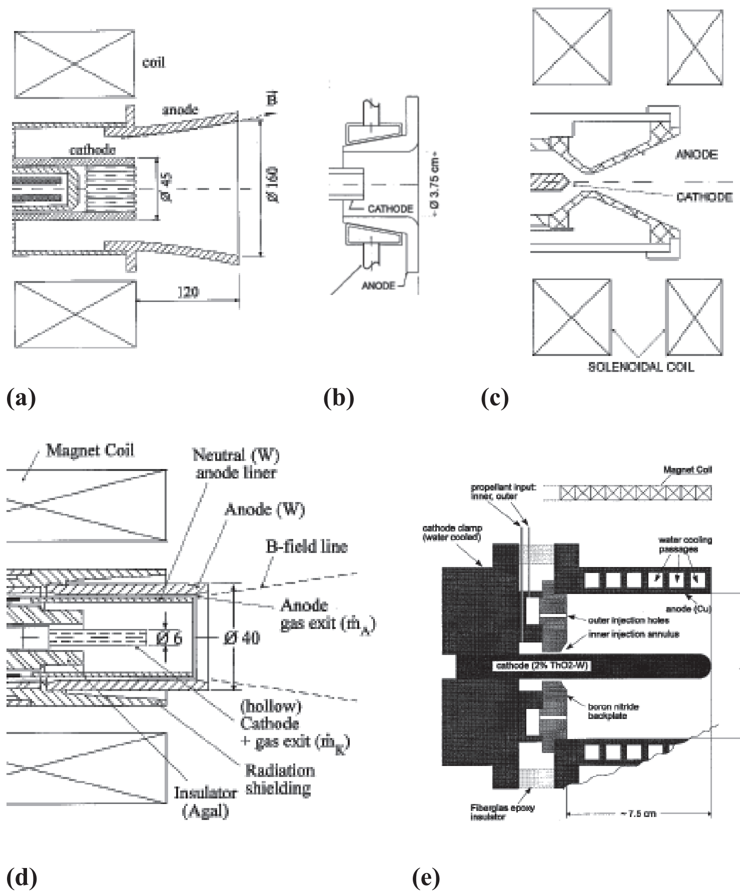

Figure 1. Various anode-cathode configurations[14].

The momentum conservation equations give a representation of the forces acting on the charged particles of type *j* in the MPD thruster and describe their motion:

$$m_j \cdot n \frac{d\overline{u}_j}{dt} = Z \cdot n_j \cdot e \cdot (\overline{E} + \overline{u}_j \times \overline{B}) - \nabla p_j + P_{jk} + f_v \tag{2}$$

Considering that the electrons mass is sensibly smaller than the one of ions, the left side inertia term is usually neglected in their motion equation, while the net viscous body forces density f_v is usually neglected for both types of particles:

$$0 = -n_e \cdot e \cdot (\overline{E} + \overline{u}_e \times \overline{B}) - \nabla p_e + P_{ei} \tag{3}$$

Here p_e and P_{ei} are the pressure and the momentum from collisions between particles of different type respectively. The same equation for ions will be the following one:

$$m_i \cdot n \frac{d\overline{u}_i}{dt} = n_i \cdot e \cdot (\overline{E} + \overline{u}_i \times \overline{B}) - \nabla p_i + P_{ie} \tag{4}$$

Considering electrical conductivity $\sigma = \frac{n_e \cdot e^2}{\nu_{ie} \cdot m_e}$ and $j = e \cdot (n_e \cdot u_e - n_i \cdot u_i)$, the momentum from collisions becomes:

$$P_{ie} = -P_{ei} = \upsilon_{ie} \cdot m_e \cdot (n_e \cdot u_e - n_i \cdot u_i) = -\frac{n_e \cdot e}{\sigma} \bar{j} \tag{5}$$

Summing up Eq. (2) and Eq. (3) and considering Eq. (4) we receive the equation of motion of both electrons and ions together:

$$m_i \cdot n \frac{d\overline{u}_i}{dt} = e \cdot \overline{E} \cdot (n_i - n_e) + n_i \cdot e \cdot (\overline{u}_i \times \overline{B}) - n_e \cdot (\overline{u}_e \times \overline{B}) - \nabla p_e - \nabla p_i = e \cdot \overline{E} \cdot (n_i - n_e) + (\bar{j} \times \overline{B}) - \nabla p \tag{6}$$

Plasma in electric propulsion is always considered to be quasi-neutral. Therefore, on the distances larger than Debye radius the electric field of one particular particle is shielded by the fields of the opposite sign particles and $n_i = n_e = n$. This leads to the vanishing of the free charge density term $e \cdot \overline{E} \cdot (n_i - n_e)$ from Eq. (5).

Part of the momentum gained by electrons from the acceleration in electric field is canceled in collisions with ions, which were also imparted with the momentum from electric field but with an opposite sign. Since electrons thermal velocity significantly exceeds ions one, there is still an essential part of the momentum from the electrons movement in electric field which accelerates the particles. In the Eq. (5) this part is represented by the $\bar{j} \times \overline{B}$ term.

Plasma moves as a unique fluid with ions electrons and neutrals exchanging momentum and energy through collisions. The difference in charged particles velocities is usually represented in the form of a current:

$$j = \sigma \cdot (\overline{E} + \overline{u}_e \times \overline{B} + \frac{1}{ne} \nabla p_e) \tag{7}$$

Considering the Hall current j_H generated in plasma due to the tensor conductivity effects and Swirl current j_S induced due to plasma diamagnetic behavior the generalized Ohm's Law takes the following form:

$$j = \sigma \cdot (\overline{E} + \overline{u}_e \times \overline{B} + \frac{1}{ne}\nabla p_e) + j_H + j_S \tag{8}$$

In the AF-MPDT, the main effect on plasma acceleration is caused by $\bar{j} \times \overline{B}$ force, which is mainly affected by applied and induced magnetic fields and pressure gradient. Therefore, the main engineering concerns are the shape and strength of applied magnetic field and geometrical nozzle shape. The shape and configuration of the electrodes are studied in the pursuit of erosion minimization, energy loss reduction in the anode potential drop and ionization efficiency increase. However, the configuration of electrons and the applied electric field may significantly affect the critical input parameters for plasma detachment from the magnetic field lines.

Unfortunately not all thruster configurations have been experimentally tested on the dependence of the electrons exhaust axial velocity on applied voltage strength and electric potential configuration. However, the applied electrical potential distribution may play a significant role on the velocity of the electrons and their ability to detach from the magnetic field lines. The electrons may even be decelerated due to the interaction with the applied electric field in the inlet and detachment zones. These factors will be discussed later. A careful study of the anode geometry may improve the performance of the magnetic nozzle and diminish the power losses.

B. Model parameters

We run the simulations using the Basic module of COMSOL Multiphysics software which uses the finite elements analyses method. At the current stage, only particles of the same charge have been studied in simulation, no collisions, no pressure term, neither Hall current nor Swirl plasma motion were taken into account. The magnetic field was chosen to be applied through two induction coils. Three types of anode-cathode configurations were examined: the anode situated significantly downstream of the cathode, Fig. 2(a), both electrodes have the same starting axial position with cylindrical anode going further downstream of the cathode region, Fig. 2(d), and same length electrodes located parallel to each other, Fig. 3(b), which will be further referred to as type I, type II and type III respectively. The particles are injected in the cathode region with their thermal velocity with electron temperature Te about 10 eV. The trajectory stream-tubes and velocities of electrons under magnetic and electric forces applied are calculated for each type and compared. The effect on the plasma plume divergence is analyzed.

In order to reduce the numerical capacity of the model the thruster was scaled 1:10, with the anode inner diameter reduced from 50 mm to 5 mm and the total thruster length from 110 mm to 11 mm. The influence of the geometry scaling on the simulation results will be analyzed in the next sub-section. The voltage applied to anode is 200A, the magnetic field strength at the axis is 0.025T. For the anode erosion prediction, the simulations with the applied magnetic field of 0.015 T are conducted for type I and type II thruster configurations.

In order to receive reasonable electron densities for particle-field interaction, the charge multiplication factor of 10^{16} was used in the particles trajectories simulation. The calculated super-particles trajectories will be further referred to as particle trajectories.

C. Results and discussion

Through the simulations we found out that the II thruster configuration has the most uniform radial distribution of the electric force. Particles in type I thruster configuration tend to be significantly more magnetized than electrons in the type II thruster configuration. The comparison between these two thruster configurations is illustrated in Fig. 2. As the electric force in the inlet region in type I thruster for all particles but central ones is directed radially, its acceleration force on the peripheral electrons is sufficiently smaller than for the central ones. This effect leads to the essential kinetic energy difference between central and peripheral particles at the thruster exit. Peripheral particles with lower axial velocity aren't able to escape from the magnetic field lines. It can be seen from Fig. 2(c) that electrons in type I thruster configuration tend to form a cone of peripheral particles with low kinetic energy and much larger plume divergence angle than the axial mainstream of plasma. This behavior was previously noticed for some regimes of AF-MPDTs.

As above mentioned, the electric field force at the exit of the thruster may also have a negative impact on the plume. Electrons may get decelerated by the reversed electric force, attracted backwards to the anode. The particles trajectories, energy and axial velocity distributions for type III thruster configuration are illustrated in Fig. 3. In order to enhance comparability, the particles for this thruster configuration were injected with an average velocity taken from the accelerated particles in the equivalent zone of the type II thruster. The comparative analyses between particles distribution in the region downstream the thruster exit for the type II thruster plotted in Fig. 3(a) and type III thruster plotted in Fig. 3(b) shows that for anode-cathode configuration III the divergent angle of the plume is higher than for the type II thruster. The only plausible explanation is that the peripheral electrons are attracted to anode backwards from the plume exhaust direction. Particles velocity reduces and they do not have enough axial momentum to escape from the curving magnetic field lines. Such plasma decelerating mechanism may explain the velocity drop with the increase of discharge current in the experiments results presented in Ref. 18.

The latter effect of the electric field distribution influencing plasma in the exit area can be significant in the case of the charge separation in the particles-magnetic field lines detachment region[19]. Under the charge separation condition the electrons will not lose the momentum gained from electric field acceleration (or deceleration) in the collisions with electrons and their trajectories will be more significantly influenced by their position in respect to the anode. Another possible case when charge separation may occur is the induction of the electron current in the near-wall region of the thruster. Besides, there might be regimes of the plasma quasi-neutrality break down. That phenomenon may happen during the stabilization process after the thruster ignition or during plasma Swirl rotation[20]. With a low mass feed rate electrons may be able to escape from more slow ions without being involved in collisions. Their interaction with the electric field configuration may be an explanation for the lower thruster efficiency in low-mass feed rate regime in the experiments results introduced in[18].

Figure 4 presents the radial distributions of the electrons velocity in the z direction (perpendicular to the simulation plane) for all three thruster configurations. All particles in the type II thruster configuration finish gyrating at approximately 1.75 s after making 1-2 rotations whereas for type I thruster the majority of electrons stop gyrating only after 4-5 rotations at 2.75-3.5 s.

In order to analyze the influence of the model geometry scaling factor, we simulated a 10:1 scaled model of the type III thruster configuration. The scaled model dimensions are considered to be of the same magnitude as the real experimentally tested MPDTs[10]. Figure 5 presents the comparison between two models. The scaling influences neither the particles trajectories distribution nor the radial distribution of the axial velocity. The maximal axial velocity in the two models at time $5x10^{-9}$s differs less than 1.7%, which is within the model error range. As shown in Fig. 5(b), in the scaled model the maximum particle velocity during the time window from $5x10^{-9}$s to $5x10^{-8}$s increases only by 0.3%. These robustness checks show that the results of the original simulation model are reasonable and represent the time window when the main electrons acceleration occurs.

The radial component of the particles acceleration force for the type I thruster configuration is smaller with respect to type II. As a consequence, the minimum applied magnetic field strength required for plume confinement and shielding of anode is sufficiently lower for type II thruster. Figure 6 illustrates the particles behavior next to anode in the weaker applied magnetic field (0.015 T) for both thruster configurations. For a better visualization of the anode contact zone, particles are considered to be frozen when hitting electrodes. A significant number of electrons hit anode in type I thruster. Conversely, in type II thruster configuration all particles are still axially confined by applied magnetic field. Hence, the anode erosion in type I geometry is higher than in type II.

The anode shape may also affect the induced currents distribution and the gas-dynamic acceleration component[12]. In order to optimize thruster geometry, further simulations taking into consideration other influence factors are required and will be considered in future developments of the present work. In another future extension of this research, we will simulate a model with two coaxial anodes axially separated from each other.

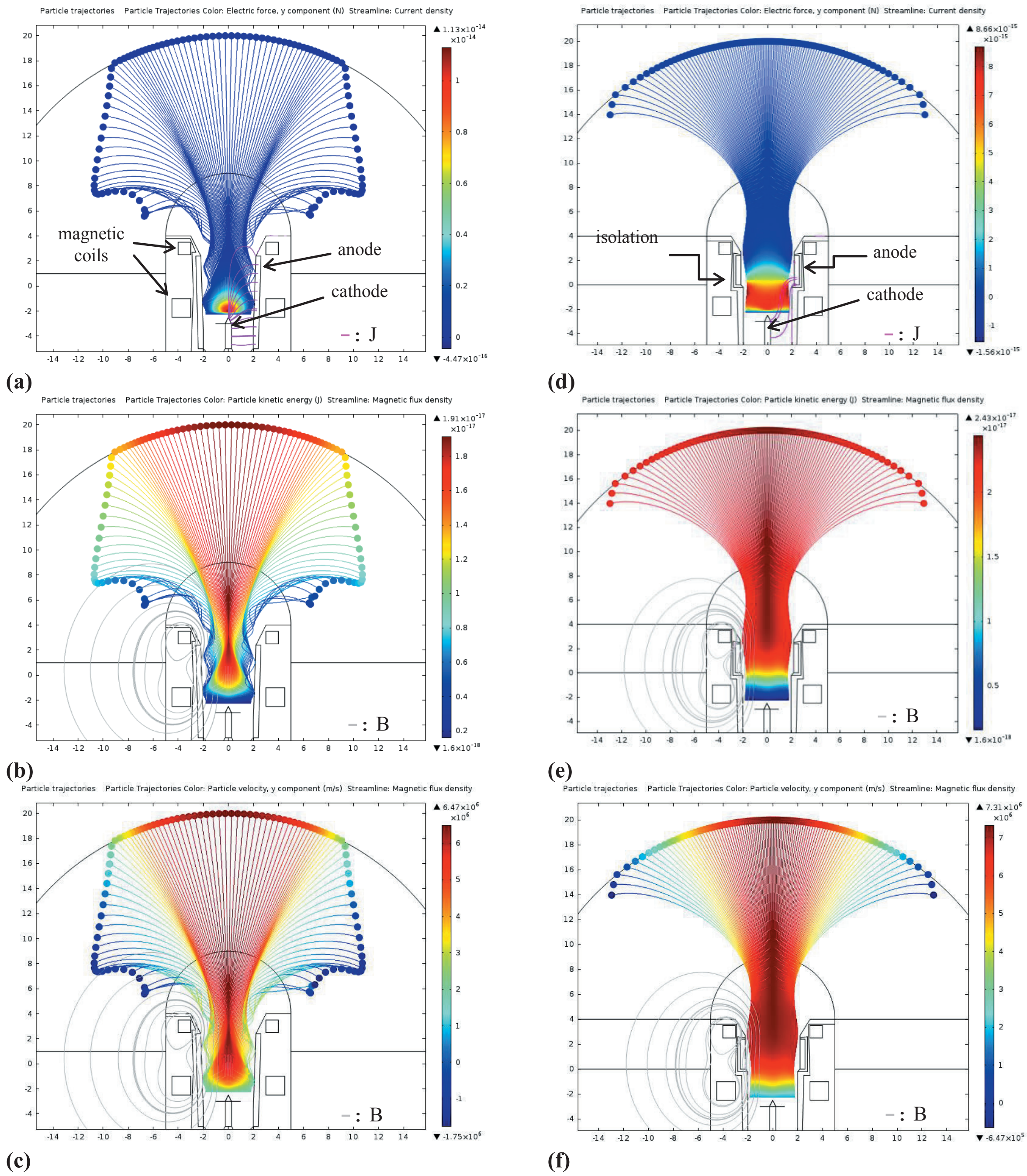

Figure 2. Particles trajectories for type I and type II axial thruster configurations, x-y scale presented in mm. (a) Axial electric force distribution for type I, (b) Kinetic energy distribution for type I, (c) Axial velocity distribution for type I, (d) Axial electric force distribution for type II, (e) Kinetic energy distribution for type II, (f) Axial velocity distribution for type II.

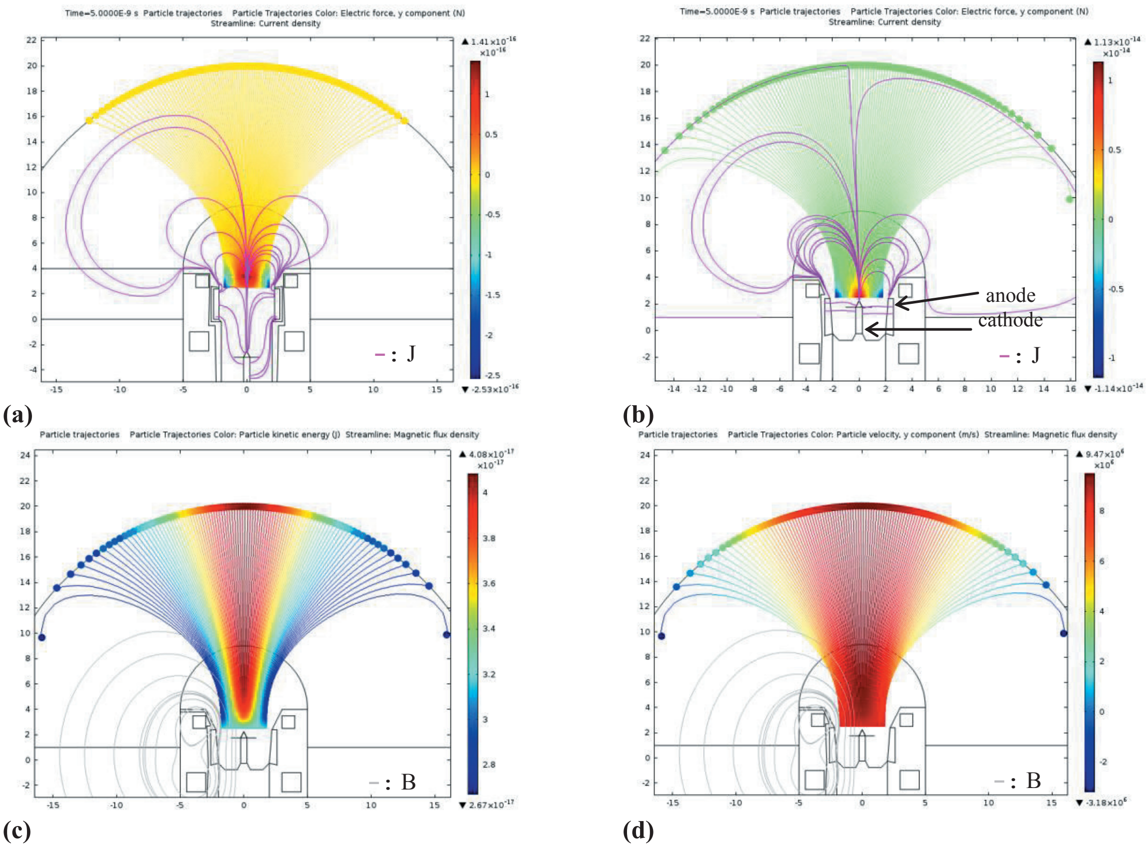

Figure 3. Particles trajectories for type II and type III thruster configurations, x-y scale presented in mm. (a) Electric force distribution for type II, (b) Electric force distribution for type III, (c) Kinetic energy distribution for type III, (d) Axial velocity distribution for type III.

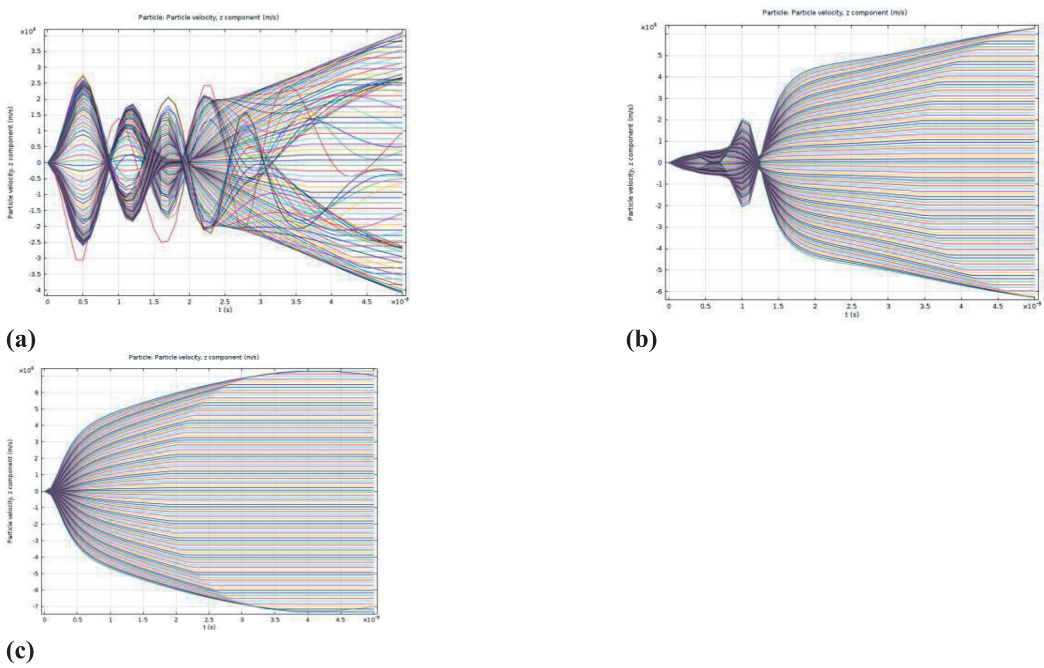

Figure 4. Each super-particle velocity z component distribution in time: (a) for type I thruster configurations, (b) for type II thruster configurations, (c) for type III thruster configurations.

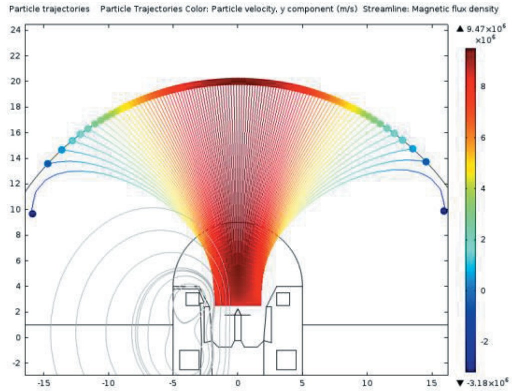

(a)

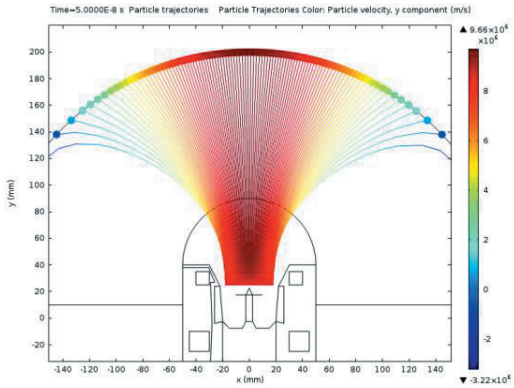

(b)

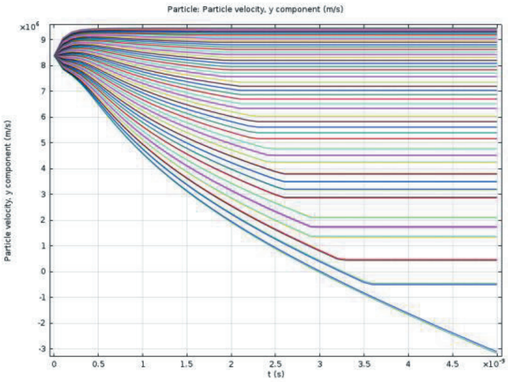

(c)

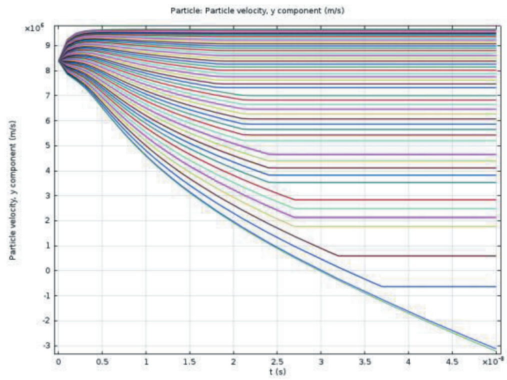

(d)

Figure 5. Type III thruster configuration: a) original model particles velocity, y component, space distribution, b) scaled 10:1 model particles velocity, y component, space distribution, c) original model particles velocity, y component, evolution in time, d) scaled 10:1 model particles velocity, y component, evolution in time.

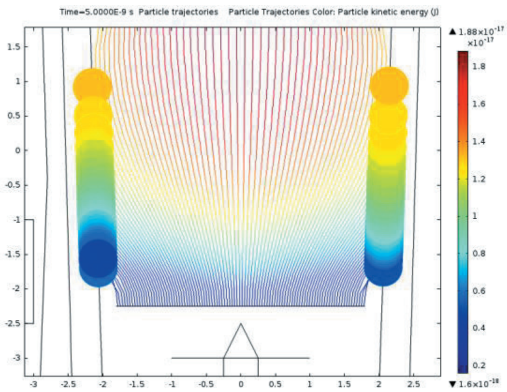

(a)

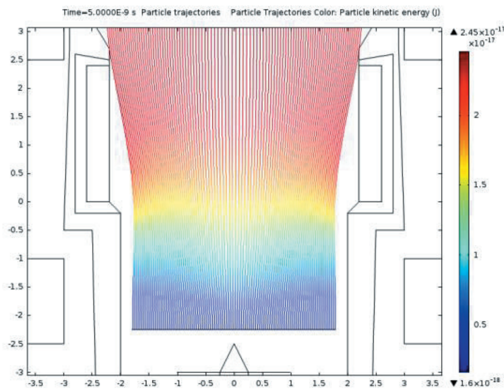

(b)

Figure 6. Particles trajectories and energy distribution in the 0.015 T applied magnetic field: a) type I thruster configuration, b) type II thruster configuration, x-y scale presented in mm.

D. Estimation of the actual electron velocity

As previously mentioned, the electric field acceleration of electrons is partially cancelled through collisions by the equivalent deceleration term of ions-electric field interaction. The electron velocity magnitude can be found from magnitudes of the current j. From Eq. 2 and Eq. 4, considering plasma quasi-neutrality the current j can be written as:

$$j = n \cdot e \cdot (\overline{u}_i - \overline{u}_e) = \sigma \cdot (\overline{E} + \overline{u}_e \times \overline{B} + \tfrac{1}{ne} \nabla p_e) \quad (9)$$

The value of current j^* in our model was calculated through the following equation:

$$j^* = -n \cdot e \cdot \overline{u}_e^{\ *} = \sigma \cdot (\overline{E} + \overline{u}_e^{\ *} \times \overline{B}) - \frac{\nabla \times \overline{B}}{\mu} \quad (10)$$

The relation between actual electrons velocity u_e and electrons velocity obtained via simulation u_e^* can be received through calculating the magnitudes of j and j^* considering u_e being co-directional with u_e^* and neglecting the electrons pressure term ∇p_e and magnetic field non-uniformity $\nabla \times \overline{B}$:

$$u_e^2 \cdot (1 + n^2 \cdot e^2) - 2 \cdot u_e \cdot (A + u_i \cdot n^2 \cdot e^2) = u_e^{*2} \cdot (n^2 \cdot e^2 - C) - 2 \cdot A \cdot u_e^* - n^2 \cdot e^2 \cdot u_i^2 \quad (11)$$

Here $A \equiv E \cdot \sigma \cdot B \cdot Sin\angle(\overline{u}_e, \overline{B}) \cdot Cos\angle(\overline{E}, [\overline{u}_e \times \overline{B}])$, $C \equiv \sigma \cdot B^2 \cdot Sin^2\angle(\overline{u}_e, \overline{B})$.

III. Conclusion

A general model of the AP-MPDT was built with examining the electrons trajectories in the applied electric and magnetic field. Since we take into consideration only some of the forces acting on plasma in the acceleration channel, the numerical values presented in this paper cannot be used as a reference. However, the general behavior of plasma illustrated in various configurations of the applied electric potential may be considered in analyzing the experimental results in specific regimes mentioned. The results of this work can be used in the engineering of the optimal anode-cathode configuration with the reduction of energy losses in the peripheral zones. The type II electrodes configuration was proved to be more efficient for the simulated case. It was also shown that this particular thruster configuration should cause less anode erosion in case of weak applied magnetic fields. Further research considering other forces acting on plasma is required. A thruster geometry with two separated anodes can also be considered.

The difference in the peripheral and axial particles velocities was explained by the shape of the electric potential distribution. This difference was suggested to be one of the reasons for efficiency losses in magnetic nozzle. The electric field decelerating effect was suggested as a possible cause of ignition instabilities and plume behavior in certain regimes observed experimentally before.

The observed tendencies in particle behavior illustrate the importance of the electric field configuration for plasma detachment problem. In the case of no-elecrodeless thrusters the whole thruster should be simulated to consider not only the magnetic field influence but also the applied electric field one. The optimal configuration of anode is suggested to be thoroughly analyzed. More tests for radial velocity distribution for various applied electric potential distribution should be performed in experimental research.

Acknowledgments

This work has been largely supported by Chinese Government and National Science Foundation of China (No. 51276006).

References

[1]Fradkin, D. B., Blackstock A. W., Roehling, D. J., Stratton, T. F., Williams, M., Liewer K. W., "Experiments Using a 25-kw Hollow Cathode Lithium Vapor MPD Arcjet", *AIAA Journal*, vol. 8, no. 5, 1970.

[2]Sutton, J., Sherman, A., *Fundamentals of Technical Magnetic Gas Dynamics*, Mir, Moscow, 1968

[3]Ahedo, E., "Parametric analysis of a magnetized cylindrical plasma," *Physics of Plasmas*, vol. 16, Nov. 2009, pp. 113503.

[4]Ahedo, E., and Merino, M., "On plasma detachment in propulsive magnetic nozzles," *Physics of Plasmas*, vol. 18, no. 5, 2011, p. 053504.

[5]Ahedo, E., and Merino, M., "Two-dimensional plasma expansion in a magnetic nozzle: Separation due to electron inertia," *Physics of Plasmas (1994-present)*, vol. 19, no. 8, Aug. 2012, p. 083501.

[6]Hooper, E. B., "Plasma detachment from a magnetic nozzle," *Journal of Propulsion and Power*, vol. 9, no.5, 1993, pp. 757–763.

[7]Breizman, B. N., Tushentsov, M. R., and Arefiev, A. V., "Magnetic nozzle and plasma detachment model for a steady-state flowa)," *Physics of Plasmas*, vol. 15, May 2008, p. 057103.
[8]Inutake, M., Ando, A., Kunihiko, H., Hiroyuki, T., Tsuyoshi, Y., "Characteristics of a Supersonic Plasma Flow in a Magnetic Nozzle", *Journal of Plasma Fusion Research*, vol.78, 2002.
[9]Winglee, R., Ziemba, T., Giersch L., Prager, J., Carscadden, J., Roberson, B. R., "Simulation and laboratory validation of magnetic nozzle effects for the high power helicon thruster", *Physics of Plasmas 14*, , 2007, 063501.
[10]Sasoh A., "Simple formulation of magnetoplasmadynamic acceleration", *Phys. Plasmas 1 (3)*, 1994.
[11]Sankaran K., Polzin, K. A., "Development of numerical tools for the investigation of plasma detachment from Magnetic Nozzle", *38-th AIAA Plasma Dynamics and Lasers Conference*, AIAA Paper, 2007-4386, Miami, FL.
[12]Kong M., Tang H., "Geometric Effects on the Acceleration Mechanisms in Applied-Field Magnetoplasmadynamic Thrusters", *The 33st International Electric Propulsion Conference*, The George Washington University, USA, 2013, IEPC-2013-115.
[13]Little, J. M., Rubin, A. S., Choueiri, E.Y., "Similarity Parameter Evolution within a Magnetic Nozzle with Applications to Laboratory Plasmas", *32nd International Electric Propulsion Conference*, Wiesbaden, Germany, 2011, IEPC-2011-229.
[14]Kruelle, G., Auweter-Kurtz, M., and Sasoh, A., "Technology and Application Aspects of Applied Field Magnetoplasmadynamic Propulsion," *Journal of Propulsion and Power*, vol. 14, no.5, 1998, pp. 754–763.
[15]Jahn, R. G., *Physics of electric propulsion*, New York: McGraw-Hill, 1968.
[16]Andrenucci, M., and Paganucci, F., "Fundamental Scaling Laws for Electric Propulsion Concepts - Part 2: MPD Thrusters," *40th AIAA/ASME/SAE/ASEE Joint Propulsion Conference and Exhibit*, AIAA, 2004.
[17]Andrenucci, M., "Magnetoplasmadynamic Thrusters," *Encyclopedia of Aerospace Engineering*, R. Blockley and W. Shyy, eds., Chichester, UK: John Wiley & Sons, Ltd, 2010.
[18]Arakawa, Y., and Sasoh, A., "Electromagnetic effects in an applied-field magnetoplasmadynamic thruster," *Journal of Propulsion and Power*, vol. 8, no. 1, 1992, pp. 98–102.
[19]Ahedo, E., and Merino, M., "Two-dimensional supersonic plasma acceleration in a magnetic nozzle," *Physics of Plasmas*, vol. 17, no. 7, 2010, p. 073501.
[20]Yoshimura S., Nagaoka K., Okamoto A., Hara K., Kono M., and Tanaka M. Y., "Potential Structure and Quasi-neutrality Breaking of Plasma Hole", *29th EPS Conference on Plasma Phys. and Contr. Fusion*, Montreux, France, ECA, vol. 26B, P-4.012, 2002.